Human Molecular Genetics, 1998, Vol. 7, No. 9 **1385–1391**

Localization of dystrophin isoform Dp71 to the inner limiting membrane of the retina suggests a unique functional contribution of Dp71 in the retina

Perry L. Howard[1,+], Ghassan Y. Dally[1,+], Melanie H. Wong[1,+], Alex Ho[1], Richard G. Weleber[2,4], De-Ann M. Pillers[3] and Peter N. Ray[1,5,*]

[1]Department of Medical and Molecular Genetics, University of Toronto, Toronto, Ontario, Canada, [2]Departments of Ophthalmology and Molecular and Medical Genetics and [3]Departments of Pediatrics and Molecular and Medical Genetics, Oregon Retinal Degeneration Center, Oregon Child Health Research Center, Doernbecher Children's Hospital, Oregon Health Sciences University, Portland, OR 97201, USA, [4]Casey Eye Institute, Oregon Health Sciences University, Portland, OR 97201, USA and [5]Departments of Genetics and Pediatric Laboratory Medicine and Research Institute, Hospital for Sick Children, 555 University Avenue, Toronto, Ontario M5G 1X8, Canada

Received March 23, 1998; Revised and Accepted June 12, 1998

The electroretinograms (ERGs) of patients with Duchenne muscular dystrophy and an allelic variant of the *mdx* mouse (*mdx*^{Cv3}) have been shown to be abnormal. Analysis of five allelic variants of the *mdx* mouse with mutations in the dystrophin gene has shown that there is a correlation between the position of the mutation and the severity of the ERG abnormality. Three isoforms are expressed in the retina: Dp427, Dp260 and Dp71. Using indirect immunofluorescence and isoform-specific antibodies on retinal sections from three allelic *mdx* mouse strains, we have examined the localization of each of the isoforms. We show that Dp71 expression does not overlap with Dp427 and Dp260 expression at the outer plexiform layer (OPL). Instead, Dp71 is localized to the inner limiting membrane (ILM) and to retinal blood vessels. Moreover, we show that Dp260 and Dp71 differ structurally at their respective C-termini. In addition, we find that the proper localization of the β-dystroglycan is dependent upon both Dp260 at the OPL and Dp71 expression at the ILM. Thus, Dp260 and Dp71 are non-redundant isoforms that are located at different sites within the retina yet have a common interaction with β-dystroglycan. Our data suggest that both Dp71 and Dp260 contribute distinct but essential roles to retinal electrophysiology.

INTRODUCTION

Duchenne muscular dystrophy (DMD) is an X-linked recessive lethal disease caused by mutations in the dystrophin gene (1–6). The gene is complex, encoding multiple tissue-specific isoforms that differ structurally in their respective N- and C-termini. Retinal electrophysiology in both humans (7–11) and mice (12; D.M. Pillers and W.R. Woodward, in preparation) with mutations in the dystrophin gene is abnormal. Analysis of dark-adapted electroretinograms (ERGs) has revealed a reduction in amplitude of the b-wave potential in the majority of DMD patients (7–11) and the dystrophic *mdx*^{Cv3} mouse (12). Characterization of ERGs from allelic variants of the *mdx* mouse and DMD/BMD patients with mutations in different regions of the dystrophin gene demonstrated a correlation between the position of the mutation (and consequently the specific dystrophin isoforms affected) and the severity of the ERG abnormality (7,10,14; D.M. Pillers and W.R. Woodward, in preparation). Mice with mutations in the 5′ end of the gene (*mdx*, *mdx*^{Cv5}) have normal ERGs, mice with mutations in the middle of the gene (*mdx*^{Cv2} and *mdx*^{Cv4}) have ERGs with increased implicit times for the b-wave and oscillatory potentials, and the *mdx*^{Cv3} mouse, with a mutation in the 3′ end of the gene, has an ERG with both increased implicit times and an attenuation of the amplitude of the b-wave response (D.M. Pillers and W.R. Woodward, in preparation). Furthermore, the targeted disruption within exon 52 of the dystrophin gene in mice results in an ERG phenotype very similar to the *mdx*^{Cv2} and *mdx*^{Cv4} mice (13). In man, DMD patients with mutations affecting the middle or 3′ end of the gene have abnormal ERGs (8–11), while most patients with mutations at the 5′ end of the gene have normal ERGs (10).

The dystrophin gene is transcribed from at least seven different promoters located in different regions of the gene. Four of these promoters are located within introns and encode short dystrophin isoforms, named according to their molecular weight. There are three full-length dystrophins (Dp427) which contain unique N-termini fused to the actin-binding, rod, cysteine-rich and C-terminal domains (14–16). Three dystrophin isoforms (Dp260, Dp140 and Dp116) lack the actin-binding domain, but contain a portion of the rod domain, and retain the cysteine-rich and C-terminal domains (17–19). The remaining isoform (Dp71) has

*To whom correspondence should be addressed. Tel: +1 416 813 6590; Fax: +1 416 813 7732; Email: peter.ray@mailhub.sickkids.on.ca
+These authors contributed equally to this work

a unique seven residue N-terminus fused to the cysteine-rich and C-terminal domains (20–24). By western blot analysis and indirect immunofluorescence, we, and others, have detected expression of three dystrophin isoforms (Dp427, Dp260 and Dp71) in the retina (7,13,17). A recent report has also suggested that Dp140 may be expressed in the retina although the localization was not determined (25). Indirect immunofluorescence analysis has shown that Dp427 and Dp260 are expressed at the outer plexiform layer (OPL) of the retina (7,17,26,27). The localization of Dp71 was not determined in these studies; however, through analysis of the exon 52 knockout mice, Kameya *et al*. deduced that Dp71 was expressed at retinal blood vessels and possibly at the inner limiting membrane (ILM) (13). The precise localization of dystrophin isoforms in the retina has been complicated by the large number of isoforms generated through multiple promoter usage, and alternative splicing of exon 78 which alters the translation reading frame and changes the hydrophilic C-terminus to a hydrophobic C-terminus (20,28,29). Isoform-specific antisera have not been available for previous studies which have relied on a combination of non-isoform-specific dystrophin antibodies and mutation information to deduce the localization of the dystrophin isoforms (7,13,17,26,27). The correlation between genotype and ERG phenotype suggests that isoform specificity is functionally important in the retina. Elucidation of these functions requires precise knowledge of the expression of individual isoforms at the cellular level. To address this issue, we have prepared isoform-specific antibodies to N-terminal regions of Dp260 (RET-1) and Dp71 (NME-1), and to the alternative C-terminus that is generated when exon 78 is spliced from the transcript (ACT-1).

The genotype–phenotype correlation supports two possible hypotheses. The dystrophin isoforms may be functionally redundant, with the severity of the phenotype increasing as the number of isoforms affected by the mutation increases, resulting in marked loss of b-wave amplitude only when all isoforms are inactivated. The relatively mild ERG phenotype seen in mdx^{Cv2}, mdx^{Cv4} and the exon 52 knockout mice could be explained by the continued expression of Dp71 which may compensate for Dp260 at the OPL. An alternative hypothesis is that the isoforms are functionally distinct and that the loss of Dp260 results in increased implicit times of the ERG while the loss of Dp71 results in reduction of b-wave amplitude. The first hypothesis implies that the subcellular localization of dystrophin isoforms should overlap, whereas the second hypothesis allows for the localization of specific isoforms to different structures.

In this report, we test these hypotheses by determining the precise localization of each isoform using isoform-specific antibodies to immunostain retinal sections of normal and dystrophic mice. We found that while the expression of Dp427 and Dp260 is restricted to the OPL, Dp71 expression is confined to the ILM and retinal blood vessels, and is absent from the OPL. We also examine β-dystroglycan expression in the mutant mice. This protein interacts with the hinge 4 and cysteine-rich region of dystrophin (30), co-localizes with dystrophin at the OPL and is also expressed at the ILM and in the retinal blood vessels (31,32). We show that β-dystroglycan localization to the OPL is dependent on the expression of Dp260, while β-dystroglycan localization at the ILM and retinal blood vessels is dependent upon Dp71 expression. Our results support the hypothesis that both Dp260 and Dp71 are required for normal electrophysiology in the retina (13; D.M. Pillers and W.R. Woodward, in preparation) and that these isoforms function at different structures in the retina through a common interaction with β-dystroglycan.

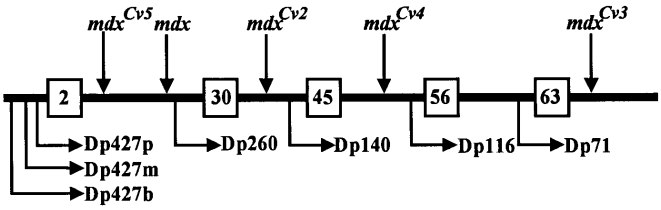

Figure 1. A diagram of the dystrophin gene indicating the positions of the dystrophin promoters (below) and the position of the mutations in each *mdx* allelic variant; adapted from Im *et al.* (33). The *mdx* mouse has a nonsense mutation in exon 23 which inactivates only Dp472 (34,35). The mdx^{Cv4} mouse has a premature stop mutation in exon 53 and expresses only Dp71 (33). The mdx^{Cv3} has a splice acceptor mutation in intron 65 of the gene and does not express any of the known isoforms (33,36).

RESULTS

Previous studies on dystrophin in the retina have utilized two mouse models, the original *mdx* and the mdx^{Cv3} mouse (11,12). We have extended this work by analysing additional mouse mutants which have been recently characterized (33). In Figure 1, we indicate the positions of the mutation in each of the *mdx* alleles along with the position of the promoters for each isoform (33–36). In this report, we determine the localization of individual isoforms by combining these genetic data with immunofluorescence analysis using isoform-specific antibodies. Table 1 summarizes the different dystrophin isoforms which are expressed in each of the mouse strains, as well as a summary of the ERG data.

Table 1. By utilizing each of the allelic strains for *mdx*, it is possible to eliminate expression of specific isoforms

	mdx^{Cv5}	*mdx*	mdx^{Cv2}	mdx^{Cv4}	mdx^{Cv3}
Dp427	–	–	–	–	–
Dp260	+	+	–	–	–
Dp140	+	+	+	–	–
Dp116	+	+	+	+	–
Dp71	+	+	+	+	–
ERG	N	N	↑IT	↑IT	↑IT ↓b-wave

In the retina, Dp427, Dp260 and Dp71 are known to be expressed. *mdx* strains (top row) retain expression of specific dystrophin isoforms. For example, the mdx^{Cv4} expresses Dp116 and Dp71 normally, but lacks expression of isoforms whose promoters are 5′ to exon 56. The ERG results are summarized (bottom row) for each of the *mdx* allelic variants. mdx^{Cv5} and *mdx* mice have normal ERGs, while mdx^{Cv2} and mdx^{Cv4} show increased b-wave implicit times and oscillatory potentials. mdx^{Cv3} has increased implicit times but also demonstrates a reduction in the b-wave amplitude. N, normal; IT, implicit time.

We prepared serial retina sections from each of the *mdx* allelic variants and examined the localization of dystrophin isoforms using antibody 1583, which recognizes the hydrophilic C-terminus. Figure 2 shows indirect immunofluorescence analysis of serial retinal sections of normal (C57BL/6J) , *mdx*, mdx^{Cv4} and mdx^{Cv3} mice. The left column (A, D, G and J) shows the

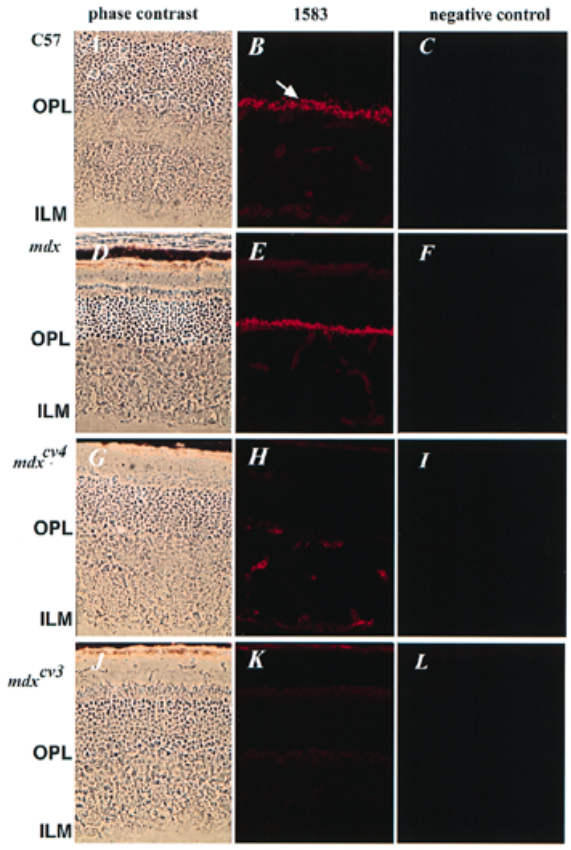

Figure 2. Serial sections of frozen retina were prepared from C57BL/6J (**A–C**), *mdx* (**D–F**), *mdx*^{Cv4} (**G–I**) and *mdx*^{Cv3} (**J–L**). The left column shows the phase-contrast image of a section. Pigment epithelium is at the top of the image and the ILM is at the bottom. The middle column shows the immunofluorescent signal obtained with 1583 on each of the different strains. A strong punctate signal (arrow) was observed at the OPL in C57BL/6J and *mdx* retina, but not in *mdx*^{Cv4} or *mdx*^{Cv3} retina. A weak signal was also detected at the ILM and retinal blood vessels in C57BL/6J, *mdx* and *mdx*^{Cv4}, which was absent in *mdx*^{Cv3}. The right-hand column shows control sections in which the primary antibody was omitted. Identical sets of controls were performed for secondary antibodies, and each of the other primary antibodies used. In all cases, no signal above background was detected.

corresponding phase-contrast micrograph of the sections. The sections are orientated such that the pigment epithelium is at the top of the image and the ILM is at the bottom. A strong punctate signal was detected at the OPL from both control and *mdx* mice (middle column B and E). This signal was absent in *mdx*^{Cv4} (H) and *mdx*^{Cv3} (K), confirming that Dp427 and Dp260 containing the hydrophilic C-terminus are expressed at the OPL. Evidence that Dp427 contributes to the immunofluorescent signal at the OPL has been demonstrated previously, using an antibody to the N-terminus of Dp427 (17). The absence of signal at the OPL in *mdx*^{Cv4} indicates that a Dp71 splice variant containing the hydrophilic C-terminus is not expressed at the OPL.

In addition to the signal at the OPL, control and *mdx* mice showed a weak signal at the ILM and retinal blood vessels. This signal was found in all of the mouse strains except *mdx*^{Cv3}, suggesting that it is due to low levels of Dp71.

To define the specific isoform expression at the ILM and retinal blood vessels in more detail, we generated several new isoform-specific antibodies. Figure 3 is a composite of retinal sections from C57BL/6J, *mdx*, *mdx*^{Cv4} and *mdx*^{Cv3} immunostained with four different antibodies. Staining with 1583 (Fig. 2) directed towards the hydrophilic C-terminus is shown in Figure 3 (A–D) for comparison. Indirect immunofluorescence staining using the hydrophobic C-terminal antibody, ACT-1, is shown in the second column (E–H). In contrast to the results with 1583, ACT-1 used on C57BL/6J and *mdx* sections showed a weak punctate signal at the OPL and a strong signal at the ILM and retinal blood vessels. No OPL signal was seen in *mdx*^{Cv4} and *mdx*^{Cv3}, indicating that Dp71 with the hydrophobic C-terminus is not expressed at the OPL. Thus, the data from *mdx*^{Cv4} using both C-terminal antibodies indicate that Dp71 is not expressed at the OPL. However, both C-terminal antibodies did detect signal at the OPL in *mdx*, indicating that there are two species of Dp260 at the OPL that differ in their respective C-termini. The strong signal using ACT-1 at the ILM and blood vessels was detected in all strains except *mdx*^{Cv3}, confirming that this signal is probably due to expression of Dp71 with the hydrophobic C-terminus.

By comparing the intensity of signal at the OPL with the intensity of signal at the ILM for antibodies 1583 and ACT-1, obvious differences in the relative amount of isoform with the two C-termini can be seen at the OPL, ILM and retinal blood vessels. More Act-1 signal was seen at the ILM and blood vessels than at the OPL. Conversely, there was more 1583 signal at the OPL than at the blood vessels and ILM. This suggests that Dp260 at the OPL contains predominantly the hydrophilic C-terminus, while Dp71 at the ILM and blood vessels contains predominantly the hydrophobic C-terminus.

To confirm that the signal we detected at the OPL was due to Dp260, and that Dp260 expression is restricted to the OPL, we used an antibody RET-1 which recognizes the unique N-terminus of Dp260. In Figure 2 (I–L), this antibody detected signal only at the OPL in C57BL/6J and *mdx* mice. As expected, no signal was found on sections from *mdx*^{Cv4} and *mdx*^{Cv3}. This confirms that Dp260 is expressed only at the OPL in the retina.

Previous reports have shown that Dp427 co-localizes with the β-dystroglycan and that the loss of dystrophin results in a concomitant loss of glycoprotein complex at the cell membrane (13,37–40). The β-dystroglycan antibody, NCL-43DAG (Novacastra, UK), clearly demonstrated the expression of β-dystroglycan at the OPL, ILM and blood vessels of retinal sections from both C57/BL6 and *mdx* mice as has been reported previously (31). While the signal at the OPL was not affected in *mdx* mice, the signal at the OPL was greatly reduced in sections from both *mdx*^{Cv4} and *mdx*^{Cv3}. These results confirm the results of Kameya *et al.* (13), indicating that Dp260 expression at the OPL is required for proper localization of β-dystroglycan. In contrast, the signal at the ILM and blood vessels appeared normal in C57Bl/6J, *mdx* and *mdx*^{Cv4} but was greatly reduced in sections from mdx^{Cv3}. Thus, the loss of both Dp427 and Dp260 is necessary to reduce β-dystroglycan localization at the OPL, while the loss of Dp71 expression at the ILM and blood vessels affects β-dystroglycan localization at these structures. In control experiments, laminin staining was unaffected in each of the strains, indicating that the reduction in signal was specific for β-dystroglycan and not due to a loss of structure (data not shown).

We have not detected the expression of Dp140 in western blot analysis of retinal extracts with any of our antisera. Thus, we conclude that the signal in the ILM and retinal blood vessels is due to Dp71 expression. However, to confirm the localization of

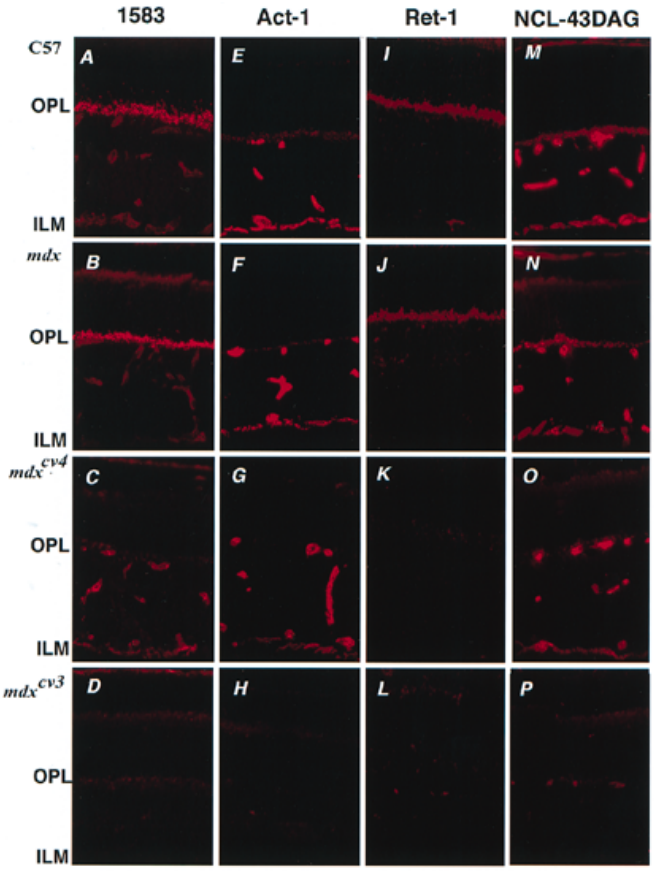

Figure 3. A composite of retinal sections from each of the different strains used in the study, comparing the signal obtained with different antibodies. The first column (**A–D**) is stained with 1583 (Fig. 2) and is shown for comparison. The second column (**E–H**) shows the immunofluorescent signal using the hydrophobic C-terminus antibody, ACT-1. A weak signal could be detected at the OPL in C57BL/6J and *mdx* that is missing in mdx^{Cv4} and mdx^{Cv3}. In contrast, a strong signal was present at the ILM and blood vessels in strains C57BL/6J, *mdx* and mdx^{Cv4} that was absent in mdx^{Cv3}. The third column (**I–L**) shows the immunofluorescent signal detected with the Dp260 N-terminus antibody RET-1. A strong signal is detected at the OPL in C57BL/6J and *mdx*, which is absent in mdx^{Cv4} and mdx^{Cv3}. No signal was detected at the ILM and blood vessels with this antibody. The fourth column (**M–P**) shows the signal using the β-dystroglycan antibody NCL-43DAG. A β-dystroglycan signal can be seen at the OPL, ILM and blood vessels in C57BL/6J and *mdx*. The OPL signal was substantially reduced at the OPL in mdx^{Cv4} but appeared to be normal at the ILM and blood vessels. In mdx^{Cv3}, all β-dystroglycan signals were greatly reduced.

Dp71 to the ILM and retinal blood vessels, we used antibody NME-1, directed against the seven amino acids encoded by exon 1 of Dp71. Since this antibody is human specific and does not recognize murine Dp71 (G.Y. Dally, unpublished data), indirect immunofluorescence analysis of serial sections from a human adult retina are shown (Fig. 4). NME-1 detected Dp71 signal only at the ILM and blood vessels, and not at the OPL. The immunostaining pattern of human retina with antibodies 1583 and ACT-1 was the same as that seen in murine retina, indicating that the localization of dystrophin isoform is identical in both species. These results confirm that the signal at the ILM and blood vessels is due to Dp71 expression in these structures.

DISCUSSION

The most severe pathological consequence of DMD is its effect on muscle tissue, which leads to progressive muscle wasting and eventual death. However, the necessity for dystrophin in the central nervous system (CNS) is also well documented (7–12,41). DMD is associated with a cognitive impairment characterized by a reduction of the mean Intelligence Quotient (IQ) (41). The dark-adapted ERG, which measures the electrophysiological response of the retina to light stimulus, is also abnormal (7–12). Thus, the retina provides a means to study the function of dystrophin in the CNS. Genotype–phenotype correlations by ERG in mouse, compared with the expression of multiple dystrophin isoforms in the retina, led to the suggestion that dystrophin isoforms have specific functions (17; D.M. Pillers and W.R. Woodward, in preparation). We have postulated that differences observed in the mouse ERGs were due to either redundant isoform expression or isoform-specific function in the retina. The purpose of this study was to test these hypotheses by establishing the localization of each dystrophin isoform using isoform-specific antisera.

Both our data and those recently published by Kameya *et al.* (13) demonstrate that Dp260 and Dp71 localize to distinct structures in the retina, with non-overlapping patterns of expression and are thus not functionally redundant. Both isoforms are required for proper b-wave formation and timing (D.M. Pillers and W.R. Woodward, in preparation). In contrast, isoform Dp427 co-localizes with Dp260 in the retina. While the finding of normal ERGs from *mdx* mice (12; D.M. Pillers and W.R. Woodward, in preparation) could suggest that Dp427 is not required for normal electrophysiology in the retina, it is also possible that Dp260 is

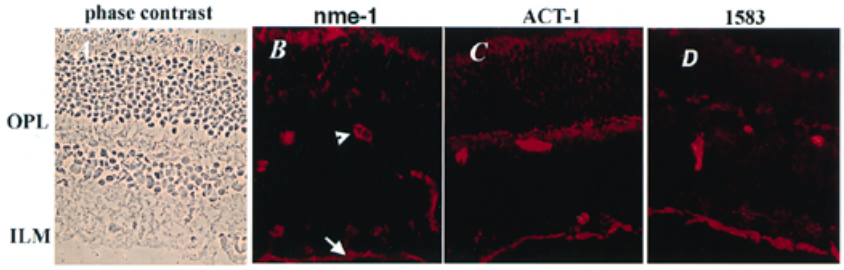

Figure 4. Serial sections from human retina were fixed and stained with Dp71 N-terminal antibody NME-1, the hydrophobic C-terminus antibody ACT-1 or the hydrophilic C-terminus antibody 1583. (**A**) A phase-contrast micrograph of a serial section indicating the location of the OPL and ILM. (**B**) NME-1 signal is detected at the ILM and blood vessels but is absent from the OPL. (**C**) ACT-1 signal is detected at the OPL, ILM and blood vessels. (**D**) 1583 signal can be detected at the OPL, ILM and blood vessels.

compensating for the loss of the Dp427 isoform. Dp260 differs from Dp427 in that it does not have the actin-binding domain at the N-terminus of the protein (17). However, recent studies have indicated the presence of an actin-binding site within exon 56 which would be present in Dp260 but not Dp71 (42). This suggests a possible interaction of Dp260 with the actin cytoskeleton analogous to that postulated for Dp427 (42). Distinguishing the role of Dp427 from Dp260 will require ERG analysis of animals with Dp260-specific mutations.

We have not been able to detect Dp140 expression in the retina by immunofluorescence or western blot analysis although it has been reported by one other group (25). The reason for this discrepancy is unknown, although it could be due to the use of different antibodies. However, no differences were found in ERG recordings between *mdx*^{Cv2} and *mdx*^{Cv4} (D.M. Pillers and W.R. Woodward, in preparation). Since *mdx*^{Cv2} expresses Dp140 while *mdx*^{Cv4} does not, it seems likely that this isoform is not required for normal electrophysiology in the retina. Unfortunately, unlike the other dystrophin isoforms, Dp140 does not encode a novel N-terminus, making the generation of Dp140-specific antibodies impossible (18). Thus, we cannot exclude the possibility that Dp140 may contribute to the expression in the retina, and that the phenotypic consequences of loss of this isoform may be masked by Dp71 expression.

We have detected a difference in the expression of the hydrophilic and hydrophobic C-termini at the OPL and ILM, with the OPL primarily expressing dystrophin with the hydrophilic C-terminus, and the ILM and retinal blood vessels primarily expressing dystrophin with the hydrophobic C-terminus. This indicates that the majority of Dp260 at the OPL, and Dp71 at the ILM and blood vessels, have different C-termini, which may influence protein–protein interactions. While the functional consequences of the splicing of exon 78 are unknown, the change introduced into the protein is significant, resulting in an overall change in hydrophobicity that seems likely to influence protein folding (20,23). Thus, the difference in expression of the C-termini at the OPL and ILM may result in distinct protein interactions at these structures.

Immunofluorescence analysis of dystrophin and β-dystroglycan expression in the retina has shown that the two proteins co-localize (31,32). Furthermore, the proper localization of β-dystroglycan to the membrane requires the expression of Dp260 at the OPL (13), and Dp71 at the ILM and blood vessels. Taken together, these data strongly indicate that both Dp260 and Dp71 participate in membrane complexes with β-dystroglycan in the retina. Analysis of β-dystroglycan and dystrophin localization in the retina by electron microscopy has shown that the proteins are found in the intracavital extensions of the presynaptic photoreceptor termini of the OPL, and the vitread membrane surface of the Muller cell endfeet which forms the ILM (32,43). The precise function of these complexes remains elusive. α- and β-dystroglycan are expressed in a wide range of tissues and, in muscle, act as a receptor for merosin and agrin in the extracellular matrix (44,45). The β-dystroglycan component binds to α-dystroglycan and spans the membrane where it interacts with dystrophin (30,44). Two models have been proposed to explain the function of dystrophin in this complex. The first is that dystrophin is required to maintain the structural integrity of the cell membrane by linking the actin cytoskeleton to the extracellular matrix (44). The second model is that dystrophin functions in a clustering process that assembles receptor membrane complexes at specialized locations on the cell surface (45,46). The first model requires an actin-binding site in dystrophin. For reasons already discussed, Dp260 could function at the OPL according to either model. However, in the case of Dp71, which lacks an actin-binding domain, it seems more likely to be involved in positioning membrane receptors according to the second model.

The non-overlapping expression patterns of Dp260 and Dp71 combined with the ERG data clearly indicate that both Dp260 at the OPL and Dp71 at the ILM and retinal blood vessels are required. In addition, both proteins appear to function through the β-dystroglycan. At present, the other protein components of the complex are unknown. From our knowledge of dystrophin function in muscle, one can speculate that these isoforms may position membrane channels or receptors at the OPL and ILM or, alternatively, are maintaining the structure of the OPL and ILM. Given the obvious differences between the OPL and ILM, it is likely that this function will involve distinct protein interactions. The identification of the proteins that associate with Dp260 at the OPL and Dp71 at the ILM and blood vessels with undoubtedly be necessary for further understanding of dystrophin function in the CNS.

MATERIALS AND METHODS

Normal human adult male retinas were obtained from the Eye Bank Laboratory of the Canadian National Institute for the Blind (Toronto, Ontario). C57BL/6J and *mdx* mice were purchased from Jackson Laboratories (Bar Harbor, ME). The *mdx*^{Cv3} and *mdx*^{Cv4} mice were supplied by Dr Verne Chapman (Roswell Park Cancer Institute, Buffalo, NY).

Antibodies

The antibody 1583 has been described previously (47). This antibody was raised against a peptide containing the last 17 amino acids of the C-terminus of dystrophin when exon 78 is included. Hydropathy profile of this C-terminus indicates that it is hydrophilic (20,28,29). Antiserum ACT-1 is specific to the alternatively spliced C-terminus that does not include exon 78, in which the 13 hydrophilic residues are replaced by 33 primarily hydrophobic ones (20,28,29). ACT-1 was generated from a peptide conjugated at its N-terminus to keyhole limpet haemocyanin (KLH): DLGRAMESLVSVMTDEEGAE-COOH (Alberta Peptide Institute, Edmonton, Canada). Antibody NME-1 was raised against a peptide (H_2N-MREQLKGG) containing the first eight amino acids of Dp71 N-terminus conjugated at its C-terminus to bovine serum albumin (BSA). Antibody RET1 was raised to a peptide (H_2N-MSARKLRNLSYKKK) containing the first 14 amino acids of the unique Dp260 N-terminus conjugated at its C-terminus to BSA. In each case, the peptides were mixed with Freund's complete adjuvant and injected into rabbits. The immune response was monitored by enzyme-linked immunosorbent assay (ELISA). Four booster injections were performed over a 6 week period before the final bleed. Serum raised to BSA-conjugated peptides was pre-purified through a column containing BSA cross-linked to Sepharose 4B (Pharmacia, PQ). Serum was isolated and purified on an affinity column in which the conjugated peptide was chemically cross-linked to CNBr-activated Sepharose 4B (Pharmacia, PQ). The specificity of each of the antibodies was confirmed by western analysis of appropri-

ate fusion proteins and the loss of signal when comparing tissue from *mdx* and *mdx*^{Cv3} mice, lacking all of the dystrophin isoforms (G.Y. Dally and P.N. Ray, in preparation).

Indirect immunofluorescence

Retinas were embedded in OCT (Miles) and flash-frozen in liquid nitrogen. Sections of 7 µm were cut using a –20°C microtome (Leica), mounted on silane-coated slides, and stored at –80°C until used. Prior to immunocytochemistry, slides were fixed with 2% formaldehyde in phosphate-buffered saline (PBS) for 15 min, treated with 0.2% sodium borohydrate (Sigma, St Louis, MO) for 15 min and permeabilized with 0.1% Triton X-100 (Sigma). Sections were washed in PBS for 10 min and blocked in 10% horse serum in PBS for 45 min. All steps were performed at room temperature.

The blocked retinal sections were rinsed briefly in PBS before addition of primary antibodies, 1583 (1:1000), ACT-1 (1:500), Ret-1 (1:1000), NME-1 (1:1000) and NCLB DAG-43 (1:50) (Novacastra). Primary antibodies were diluted in 1% horse serum, 1% fetal calf serum, 0.03% BSA in PBS. Sections were incubated with primary antibody for 2 h, and washed for 10 min three times in PBS. Secondary antibodies consisted of either a biotin-conjugated anti-rabbit IgG (to detect 1583, Act-1, Ret-1, NME-1) or a biotin-conjugated anti-mouse IgG (to detect NCL-BDAG-43) and were incubated with the sections for 1 h at room temperature. The slides were washed three times with PBS before being incubated with rhodamine conjugated to streptavidin (diluted 1:100) (Jackson Immunoresearch, Westgrove, PA) for 1 h. Sections were washed in PBS, mounted in Immunoflo (ICN) and examined using a Leica epifluorescent microscope with rhodamine filter. Negative controls were treated in an identical manner except for the omission of the primary or secondary antibodies.

ACKNOWLEDGEMENTS

The authors would like to thank Iris Diplock in the Department of Pathology (Hospital for Sick Children) for preparing the retina sections. We are grateful to Danka Vidgen and Dr Carol Freund for their helpful discussions. This work was supported by the Medical Research Council of Canada (P.N.R.), Research to Prevent Blindness (R.G.W.), Foundation Fighting Blindness (D.M.P.) and NIH EY10084 (D.M.P.). P.L.H. was the recipient of an Ontario Graduate Scholarship.

REFERENCES

1. Burghes, A.H.M., Logan, C., Hu, X., Belfall, B., Worton, R.G. and Ray, P.N. (1987) A cDNA clone from the Duchenne/Becker muscular dystrophy gene. *Nature*, **328**, 434–437.
2. Hoffman, E.P., Brown, R.H.J. and Kunkel, L.M. (1987) Dystrophin: the protein product of the Duchenne muscular dystrophy locus. *Cell*, **51**, 919–928.
3. Koenig, M., Hoffman, E.P., Bertelson, C.J., Monaco, A.P., Feener, C. and Kunkel, L.M. (1987) Complete cloning of the Duchenne muscular dystrophy (DMD) cDNA and preliminary genomic organization of the DMD gene in normal and affected individuals. *Cell*, **50**, 509–517.
4. Kunkel, L.M. (1986) Analysis of deletions in DNA from patients with Becker and Duchenne muscular dystrophy. *Nature*, **322**, 73–77.
5. Monaco, A.P., Bertelson, C.J., Liechti Gallati, S., Moser, H. and Kunkel, L.M. (1988) An explanation for the phenotypic differences between patients bearing partial deletions of the DMD locus. *Genomics*, **2**, 90–95.
6. Monaco, A.P., Neve, R.L., Colletti Feener, C., Bertelson, C.J., Kurnit, D.M. and Kunkel, L.M. (1986) Isolation of candidate cDNAs for portions of the Duchenne muscular dystrophy gene. *Nature*, **323**, 646–650.
7. Pillers, D.M., Bulman, D.E., Weleber, R.G., Sigesmund, D.A., Musarella, M.A., Powell, B.R., Murphey, W.H., Westall, C., Panton, C., Becker, L.E. *et al*. (1993) Dystrophin expression in the human retina is required for normal function as defined by electroretinography. *Nature Genet*., **4**, 82–86.
8. De Becker, I., Riddell, D.C., Dooley, J.M. and Tremblay, F. (1994) Duchenne muscular dystrophy: negative scotopic bright-flash electroretinogram and normal dark adaptation. *Can. J. Ophthalmol*., **29**, 280–283.
9. Fitzgerald, K.M., Cibis, G.W., Giambrone, S.A. and Harris, D.J. (1994) Retinal signal transmission in Duchenne muscular dystrophy—evidence for dysfunction in the photoreceptor depolarizing bipolar cell pathway. *J. Clin. Invest*., **93**, 2425–2430.
10. Sigesmund, D.A., Weleber, R.G., Pillers, D.M., Westall, C.A., Panton, C.M., Powell, B.R., Heon, E., Murphey, W.H., Musarella, M.A. and Ray, P.N. (1994) Characterization of the ocular phenotype of Duchenne and Becker muscular dystrophy. *Ophthalmologica*, **101**, 856–865.
11. Cibis, G.W., Fitzgerald, K.M., Harris, D.J., Rothberg, P.G. and Rupani, M. (1993) The effects of dystrophin gene mutations on the ERG in mice and humans. *Invest. Ophthalmol. Vis. Sci*., **34**, 3646–3652.
12. Pillers, D.M., Weleber, R.G., Woodward, W.R., Green, D.G., Chapman, V.M. and Ray, P.N. (1995) *mdx*^{Cv3} mouse is a model for electroretinography of Duchenne/Becker muscular dystrophy. *Invest. Ophthalmol. Vis. Sci*., **36**, 462–466.
13. Kameya, S., Araki, E., Katsuki, M., Mizota, A., Adachi, E., Nakahara, K., Nonaka, I., Sakurage, S., Takeda, S. and Nabeshima, Y. (1997) Dp260 disrupted mice revealed prolonged implicit time of the b-wave in ERG and loss of accumulation of β-dystroglycan in the outer plexiform layer in the retina. *Hum. Mol. Genet*., **6**, 2195–2203.
14. Boyce, F.M., Beggs, A.H., Feener, C. and Kunkel, L.M. (1991) Dystrophin is transcribed in brain from a distant upstream promoter. *Proc. Natl Acad. Sci. USA*, **88**, 1276–1280.
15. Gorecki, D., Monaco, A., Derry, J., Walker, A., Barnard, E. and Barnard, P. (1992) Expression of four alternative dystrophin transcripts in brain regions regulated by different promoters. *Hum. Mol. Genet*., **1**, 505–510.
16. Holder, E., Maeda, M. and Bies, R.D. (1996) Expression and regulation of the dystrophin Purkinje promoter in human skeletal muscle, heart, and brain. *Hum. Genet*., **97**, 232–239.
17. D'Souza, V.N., Nguyen, T.M., Morris, G.E., Karges, W., Pillers, D.M. and Ray, P.N. (1995) A novel dystrophin isoform is required for normal retinal electrophysiology. *Hum. Mol. Genet*., **4**, 837–842.
18. Lidov, H.G., Selig, S. and Kunkel, L.M. (1995) Dp140: a novel 140 kDa CNS transcript from the dystrophin locus. *Hum. Mol. Genet*., **4**, 329–335.
19. Byers, T.J., Lidov, H.G. and Kunkel, L.M. (1993) An alternative dystrophin transcript specific to peripheral nerve. *Nature Genet*., **4**, 77–81.
20. Lederfein, D., Levy, Z., Augier, N., Mornet, D., Morris, G., Fuchs, O. and Yaffe, D. (1992) A 71-kilodalton protein is a major product of the Duchenne muscular dystrophy gene in brain and other nonmuscle tissues. *Proc. Natl Acad. Sci. USA*, **89**, 5346–5350.
21. Lederfein, D., Yaffe, D. and Nudel, U. (1993) A housekeeping type promoter, located in the 3′ region of the Duchenne muscular dystrophy gene, controls the expression of Dp71, a major product of the gene. *Hum. Mol. Genet*., **2**, 1883–1888.
22. Hugnot, J.P., Gilgenkrantz, H., Vincent, N., Chafey, P., Morris, G., Monaco, A., Berwald-Netter, Y., Koulakoff, A., Kaplan, J.C., Kahn, A. *et al*. (1992) Distal transcript of the dystrophin gene initiated from an alternative first exon and encoding a 75 kDa protein widely distributed in nonmuscle tissues. *Proc. Natl Acad. Sci. USA*, **89**, 7506–7510.
23. Bar, S., Barnea, E., Levy, Z., Neuman, S., Yaffe, D. and Nudel, U. (1990) A novel product of the Duchenne muscular dystrophy gene which greatly differs from the known isoforms in its structure and tissue distribution. *Biochem. J*., **272**, 557–560.
24. Blake, D., Love, D., Tinsley, J., Morris, G., Turley, H., Gatter, K., Dickson, G., Edwards, Y. and Davies, K. (1992) Characterization of a 4.8 kb transcript from the Duchenne muscular dystrophy locus expressed in Schwannoma cells. *Hum. Mol. Genet*., **1**, 103–109.
25. Rodius, F., Claudepierre, T., Rosasvargas, H., Cisneros, B., Montanez, C., Dreyfus, H., Mornet, D. and Rendon, A.(1997) Dystrophins in developing retina—Dp260 expression correlates with synaptic maturation. *Neuroreport*, **8**, 2383–2387.
26. Schmitz, F., Holbach, M. and Drenckhahn, D. (1993) Colocalization of retinal dystrophin and actin in post-synaptic dendrites of rod and cone photoreceptor synapses. *Histochemistry*, **100**, 473–479.

27. Miike, T., Miyatake, M., Zhao, J., Yoshioka, K. and Uchino, M. (1989) Immunohistochemical dystrophin reaction in synaptic regions. *Brain Dev.*, **11**, 344–346.
28. Bies, R.D., Phelps, S.F., Cortez, M.D., Roberts, R., Caskey, C.T. and Chamberlain, J.S. (1992) Human and murine dystrophin mRNA transcripts are differentially expressed during skeletal muscle, heart, and brain development. *Nucleic Acids Res.*, **20**, 1725–1731.
29. Feener, C.A., Koenig, M. and Kunkel, L.M. (1989) Alternative splicing of human dystrophin mRNA generates isoforms at the carboxy terminus. *Nature*, **338**, 509–511
30. Jung, D., Yang, B., Meyer, J., Chamberlain, J.S. and Campbell, K.P. (1995) Identification and characterization of the dystrophin anchoring site on beta-dystroglycan. *J. Biol. Chem.*, **270**, 27305–27310.
31. Montanaro, F., Carbonetto, S., Campbell, K.P. and Lindenbaum, M. (1995) Dystroglycan expression in the wild type and *mdx* mouse neural retina: synaptic co-localization with dystrophin, dystrophin-related protein but not laminin. *J. Neurosci. Res.*, **42**, 528–538.
32. Schmitz, F. and Drenckhahn, D. (1997) Localization of dystrophin and β-dystroglycan in bovine retinal photoreceptor processes extending into the post-synaptic dendritic complex. *Histochem. Cell Biol.*, **108**, 249–255.
33. Im, W.B., Phelps, S.F., Copen, E.H., Adams, E.G., Slightom, J.S. and Chamberlain, J.S. (1996) Differential expression of dystrophin isoforms in strains of *mdx* mice with different mutations. *Hum. Mol. Genet.*, **5**, 1149–1153.
34. Bulfield, G., Siller, W.G., Wight, P.A.L. and Moore, K.J. (1984) X chromosome-linked muscular dystrophy (*mdx*) in the mouse. *Proc. Natl Acad. Sci. USA*, **81**, 1189–1192.
35. Ryder Cook, A.S., Sicinski, P., Thomas, K., Davies, K.E., Worton, R.G., Barnard, E.A., Darlison, M.G. and Barnard, P.J. (1988) Localization of the *mdx* mutation within the mouse dystrophin gene. *EMBO J.*, **7**, 3017–3021.
36. Cox, G., Phelps, S., Chapman, V. and Chamberlain, J. (1993) New *mdx* mutation disrupts expression of muscle and non-muscle isoforms of dystrophin. *Nature Genet.*, **4**, 87–93.
37. Ervasti, J.M., Ohlendieck, K., Kahl, S.D., Gaver, M.G. and Campbell, K.P. (1990) Deficiency of a glycoprotein component of the dystrophin complex in dystrophic muscle. *Nature*, **345**, 315–319.
38. Greenberg, D.S., Schatz, Y., Levy, Z., Pizzo, P., Yaffe, D. and Nudel, U. (1996) Reduced levels of dystrophin associated proteins in the brains of mice deficient for Dp71. *Hum. Mol. Genet.*, **5**, 1299–1303.
39. Ohlendieck, K. and Campbell, K.P. (1991) Dystrophin-associated proteins are greatly reduced in skeletal muscle from *mdx* mice. *J. Cell Biol.*, **115**, 1685–1694.
40. Matsumura, K. and Campbell, K.P. (1993) Deficiency of dystrophin-associated proteins: a common mechanism leading to muscle cell necrosis in severe childhood muscular dystrophies. *Neuromusc. Disord.*, **3**, 109–118.
41. Emery, A.E. (1989) Clinical and molecular studies in Duchenne muscular dystrophy. *Prog. Clin. Biol. Res.*, **306**, 15–28.
42. Rybakova, I.N., Amann, K.J. and Ervasti, J.M. (1996) A new model for the interaction of dystrophin with F-actin. *J. Cell Biol.*, **135**, 661–672.
43. Ueda, H., Kabayashi, T., Mitsui, K., Tsurugi K., Tsukahara, S. and Ohno, S. (1995) Dystrophin localization at presynapse in rat retina revealed by immunoelectron microscopy. *Invest. Ophthalmol. Vis. Sci.*, **36**, 2318–2322.
44. Ibraghimov Beskrovnaya, O., Ervasti, J.M., Leveille, C.J., Slaughter, C.A., Sernett, S.W. and Campbell, K.P. (1992) Primary structure of dystrophin-associated glycoproteins linking dystrophin to the extracellular matrix. *Nature*, **355**, 696–702.
45. Sealock, R., Butler, M.H., Kramarcy, N.R., Gao, K.X., Murnane, A.A., Douville, K. and Froehner, S.C. (1991) Localization of dystrophin relative to acetylcholine receptor domains in electric tissue and adult and cultured skeletal muscle. *J. Cell Biol.*, **113**, 1133–1144.
46. Campanelli, J.T., Roberds, S.L., Campbell, K.P. and Scheller, R.H. (1994) A role for dystrophin-associated glycoproteins and utrophin in agrin-induced AChR clustering. *Cell*, **77**, 663–674.
47. Bulman, D.E., Murphy, E.G., Zubrzycka-Gaarn, E.E., Worton, R.G. and Ray, P.N. (1991) Differentiation of Duchenne and Becker muscular dystrophy phenotypes with amino- and carboxy-terminal antisera specific for dystrophin. *Am. J. Hum. Genet.*, **48**, 295–304.